Computers in Industry 155 (2024) 104058

Contents lists available at ScienceDirect

Computers in Industry

journal homepage: www.sciencedirect.com/journal/computers-in-industry

# Training of physics-informed Bayesian neural networks with ABC-SS for prognostic of Li-ion batteries☆

Juan Fernández [a,b,*], Matteo Corbetta [b], Chetan S. Kulkarni [b], Juan Chiachío [a], Manuel Chiachío [a]

[a] Department of Structural Mechanics and Hydraulic Engineering, Andalusian Research Institute in Data Science and Computational Intelligence (DaSCI), University of Granada (UGR), Granada 18001, Spain

[b] KBR, Inc., NASA Ames Research Center, Moffett Field, 94035, CA, United States of America

ARTICLE INFO

*Keywords:*
Physics-informed neural networks
Bayesian training
Prognostics
Uncertainty quantification
Li-ion batteries

ABSTRACT

The current surge in the need for Li-ion batteries to power electric vehicles has also translated in a need for more advanced models that can predict their behavior, but also quantify the uncertainty in their predictions, given the amount of variables involved and the varying operating conditions. This manuscript proposes a new Bayesian physics-informed recurrent neural network, where the battery discharge curve is described using the Nernst and Butler–Volmer equations, the activity correction term within such equations is modeled with two multilayer perceptrons, and approximate Bayesian computation by subset-simulation is used to train the weights, bias and the physical parameters representing the maximum charge available and the internal resistance. The challenges found during the adaptation and implementation of the Bayesian training algorithm to the recurrent physics-informed cell are described, along with the approaches proposed to overcome them. The performance of the Bayesian hybrid model presented in this paper has also been evaluated using data from NASA Ames Prognostics Data Repository, and the results show comparable accuracy to the standard approach with backpropagation, and a flexible and realistic quantification of the uncertainty. Furthermore, the uncertainty related to the physical parameters of the hybrid model can be evaluated in semi-isolation of the weights and bias of the MLPs, providing a sensitivity tool to assess the relative importance between different parameters.

## 1. Introduction

The importance of electrical batteries in modern society is undoubted, and their demand is increasing at a fast pace, from about 700 GWh in 2022 to around 4.7 TWh by 2030, according to *"Battery 2030: Resilient, sustainable, and circular"* a report elaborated by McKinsey (Fleischmann et al., 2023). Some of the reasons for this growth is the key role that they play in enabling the integration of renewable energy sources into the power grid, by storing the excess energy that is generated during periods of high production and releasing it when renewable sources are not generating electricity. However, it is foreseen that the vast bulk of such demand will come from electric vehicles (EVs), from cars to unmanned aerial vehicles (UAVs), where batteries provide the energy needed for propulsion and the operation of their systems (Diampovesa et al., 2021). This is also the case in the field of space exploration, where satellites, spacecraft, and rovers use them to control a wide range of instruments (Berri et al., 2021). Therefore, there is a need for new and more advanced models that enable us to monitor the health of the battery in real-time, but also predict their performance (Petrillo et al., 2020). The end-of-discharge (EOD) of a battery is subject to multiple factors, such as unpredictable changes in environmental conditions, thus quantifying the uncertainty in the predictions can be crucial.

Different electrochemical models can be found in the literature, which provide a robust tool to understand and predict the performance of Li-ion batteries. Among them, Doyle et al. (1993) modeled the galvanostatic charge and discharge of a full cell using concentrated solution theory. Ning and Popov (2004) proposed a charge–discharge model to simulate the capacity fade of Li-ion batteries, based on the reduction of active lithium ions and the rise of the anode film resistance. Rong and Pedram (2006) developed an analytical formulation

☆ Source of support: This paper is part of the ENHAnCE project, which has received funding from the European Union's Horizon 2020 research and innovation programme under the Marie Skłodowska-Curie grant agreement No 859957. The authors would like to thank the System-Wide Safety project and the Diagnostics and Prognostics Group at NASA Ames Research Center for the resources provided.

* Corresponding author at: Department of Structural Mechanics and Hydraulic Engineering, Andalusian Research Institute in Data Science and Computational Intelligence (DaSCI), University of Granada (UGR), Granada 18001, Spain.

*E-mail address:* juanfdez@ugr.es (J. Fernández).

https://doi.org/10.1016/j.compind.2023.104058
Received 19 September 2023; Received in revised form 2 November 2023; Accepted 28 November 2023
Available online 8 December 2023

for predicting the EOD of a lithium-ion battery, based on current and voltage measurements and taking into account the temperature and aging effects. Karthikeyan et al. (2008) presented a framework to describe the equilibrium potential as a function of the concentration, based on thermodynamic principles. Those type of models have proven to be accurate, but at the expense of being computationally costly given the differential equations that need to be solved. M. Daigle and C. Kulkarni proposed a electro-chemical model in Daigle and Kulkarni (2013) that can be run in-time for diagnostic applications and time to discharge predictions. The proposed method presented in this manuscript is built upon the principles of such model, and further information can be found in Section 2.1.

Data-driven methods have also been applied extensively to prediction of EOD and remaining useful life (RUL) in Li-ion batteries (Venugopal et al., 2021; Cheng et al., 2020; Tang and Yuan, 2022). However, these methods require great amounts of data for training, and extrapolation performance is often an issue (Haley and Soloway, 1992). Hence, new methods which combine physics-based models and data-driven algorithms have appeared in the recent years. Among those, physics-informed neural networks (PINNs) have provided promising results. For example, Shi et al. (2022) combined physics-based degradation models with LSTM neural networks into a hybrid model to predict the degradation behavior and the RUL of Li-ion batteries under different operating and environmental conditions. More in line with the work of Raissi et al. in Raissi et al. (2019), Wen et al. (2023) fused semi-empirical partial differential equations with neural networks to model the degradation behavior of Li-ion batteries, including an uncertainty-based weighting method to balance the different learning tasks during training. Similarly, S. Singh et al. proposed introducing the PDE of Fick's law of diffusion into the training process of a neural network, to predict not only the state of charge but also the state of health of Li-ion batteries. A completely different approach can be found in Nascimento et al. (2021), where R.G. Nascimento et al. presented a recurrent cell, with an architecture that resembles LSTM networks, which includes the equations in Daigle and Kulkarni (2013) in a recursive manner, but where the non-ideal voltage correction is modeled using two multilayer perceptrons (MLPs). This hybrid model also takes into account the aging effect by modeling the decrease in the total available charge and the increase of the internal resistance. Furthermore, the uncertainty in its predictions is quantified by using variational Bayesian layers, and an ensemble of different MLPs to capture the inter-specimen variability. However, this method is subject to the drawbacks of variational inference and the backpropagation algorithm, which may also result in a rigid quantification of the uncertainty due to the use of predefined probability density functions to describe the weights.

This manuscript proposes a new Bayesian PINN to model the EOD of Li-ion batteries, which combines and adapts the physics proposed in Daigle and Kulkarni (2013), the recurrent architecture proposed in Nascimento et al. (2021), and the Bayesian training proposed in Fernández et al. (2022). The non-parametric formulation of the weights, the absence of likelihood function and the gradient-free nature of approximate Bayesian computation by subset simulation (ABC-SS) provides a flexible and realistic quantification of the uncertainty. However, the use of ABC-SS as the training algorithm also poses a series of challenges, which are described in the following sections, along with the proposed solutions. The performance of this Bayesian hybrid algorithm is evaluated using a publicly available battery usage data set from NASA AMES Prognostics Data Repository (Saha and Goebel, 2007; Bole et al., 2014).

The remaining of this manuscript is organized as follows. Section 2 provides the foundations on which the proposed methodology is based. Section 3 presents the proposed hybrid algorithm including the challenges and solutions found during pre-training, training and testing stages, as well as the results of the experiments. Finally, the conclusions obtained are given in Section 4.

## 2. Background

This section presents the fundamental principles on which this manuscript is based, from physics-based electrochemical models, to physics-informed neural networks and the Bayesian approach to training.

### 2.1. Lithium-ion battery physics-based model

Lithium-ion battery physics-based models are mathematical representations which attempt to describe the chemical reactions that take place at the positive and negative electrodes inside the batteries during the charge and discharge phases, including their electrical performance under different operating conditions, based on the fundamental principles of physics. These models also incorporate the movement of lithium ions between the electrodes and electrolyte solution, which is critical for understanding the battery's behavior.

More specifically, this manuscript is based upon the principles described in Daigle and Kulkarni (2013), where M. Daigle and C. Kulkarni proposed a new electrochemistry-based model for monitoring, diagnosis and prognosis purposes. This model aims at predicting the end-of-discharge, which occurs when the voltage reaches a defined value, also known as the cut-off voltage. To this end, the voltage in the battery is modeled as a function of two different variables, namely time and the current drawn from the battery at each precise time-step. Hence, the model has a recursive nature, where data about the current drawn from the battery is fed into the model sequentially throughout all time-steps. Given that the final goal is the application of the model to prognostics, the lumped-parameter ordinary differential equations form was used, as they are more efficient for this type of tasks.

In this model, the voltage of the battery at a given time step $V(t)$ is defined by the difference between the potential at the positive and negative current collectors, and then deducting the resistance losses at each of the collectors, as per Eq. (1).

$$V = V_{U,p} - V_{U,n} - V_o - V_{\eta,p} - V_{\eta,n} \tag{1}$$

The voltage at any time-step depends on the equilibrium potential in both the positive $V_{U,p}$ and negative $V_{U,n}$ collectors, the drops caused by the electrolyte ohmic resistance, the solid-phase ohmic resistances including those at the current collectors (which are combined into a lumped constant $R_0$ used to compute $V_o$), and the surface overpotentials $V_{\eta,p}$ and $V_{\eta,n}$ coming from the solid-electrolyte interface (SEI) kinetics and the charge transfer resistance (described by the Butler-Volmer equation). The equilibrium potential, expressed in Eq. (2), includes the non-ideal voltage expressed as the activity coefficient term $V_{INT,i}$ (Karthikeyan et al., 2008), shown in Eq. (3) (null for ideal conditions). The latter is related to excess Gibbs free energy and defined by the Redlich–Kister expansion where the parameters $A_{i,k}$ were, in the original work, fitted using the Nelder–Mead simplex method and real data.

$$V_{U,i} = U_0 + \frac{RT}{nF} \ln\left(\frac{1 - x_i}{x_i}\right) + V_{INT,i} \tag{2}$$

$$V_{INT,i} = \frac{1}{nF}\left(\sum_{k=0}^{N_i} A_{i,k}\left((2x_i - 1)^{k+1} - \frac{2x_i k(1 - x_i)}{(2x_i - 1)^{1-k}}\right)\right) \tag{3}$$

The resulting model was then originally introduced in a model-based prognostics architecture (Daigle and Goebel, 2012), which comprises of an estimation problem to define the joint state-parameter estimate based on previous observations, and the prediction problem to identify the end of discharge. Finally, battery aging was also evaluated, observing that model predictions could be adapted to describe such aging by an increase of the internal resistance $R_o$ and a decrease of the total available charge $q_{max}$.

### 2.2. Physics-informed recurrent cell

Physics-based models, such as the one presented in Section 2.1, can provide valuable insights about how the system works and its fundamental properties (Coll and Lajium, 2011). At the other end of the spectrum, data-driven algorithms can make predictions based on patterns and correlations found in large data sets (Vaish et al., 2021). Moreover, they may uncover complex relationships and patterns that may be challenging for humans to describe as mathematical formulations. Therefore, in those situations where the underlying physics is uncertain or very expensive to compute, and there is a certain amount of real data available, the combination of data-driven and physics-based models into a hybrid algorithm may provide a clear advantage. To that end, and mainly based on Yucesan and Viana (2021), Nascimento et al. presented a hybrid physics-informed neural network to forecast the remaining useful life of Li-ion batteries (Nascimento et al., 2021), using the physics presented in Section 2.1 and Daigle and Kulkarni (2013), and real data from NASA Ames Prognostics Data Repository (Saha and Goebel, 2007; Bole et al., 2014).

This hybrid model comprises of a recurrent cell where physics is coded in the form of a non-linear ordinary differential equation, allowing for a state update per time step. Thus, the resulting recurrent cell updates the state vector at time $t$, given by $h_t$, based on the state vector at the previous time step $h_{t-1}$ and the input information $u_t$ at the present time-step. The recurrent model produces one-step-ahead predictions, given by $y_t$, throughout all time-steps. This recursive forward pass is described in Eq. (4), and the recurrent cell containing the physics is shown in Fig. 1, originally presented in Nascimento et al. (2021).

$$h_t = g_1(u_t, h_{t-1}) \qquad \text{and} \qquad y_t = g_2(h_t) \tag{4}$$

The activity correction terms $V_{INT,i}$, computed with a polynomial expansion in Eq. (3) (defined $V_{ni,i}$ in Nascimento et al. (2021)) are substituted by two multi-layer perceptrons (MLPs) as per Eq. (5), where $w$, $b$ are weights and biases, and the input to the MLPs is given by the mole fractions $x_p$ and $x_n$. The internal resistance $R_o$ and the total available charge $q_{max}$ are modeled as trainable parameters within the hybrid recurrent neural network, so the aging process of the battery can also be taken into account. Finally, uncertainty about the inter-battery variability was evaluated using K-fold cross-validation, and the uncertainty regarding battery aging was assessed through an ensemble of variational Bayesian layers coded with *Tensorflow* (Abadi et al., 2015).

$$V_{ni,p} = MLP_p(x_p, w_p, b_p) \qquad \text{and} \qquad V_{ni,n} = MLP_n(x_n, w_n, b_n) \tag{5}$$

This hybrid model was tested in several experiments about predicting the voltage discharge curve with constant and random loading. The flexibility of the MLPs to correct for missing physics was evident, and the aging effect was also successfully captured using variational multi-layer perceptrons. The model was trained with backpropagation (Rumelhart et al., 1986).

### 2.3. Bayesian neural networks trained with ABC-SS

Bayesian neural networks (BNN) are a probabilistic approach to training artificial neural networks (ANN). Contrary to standard ANNs, which use the backpropagation algorithm (Rumelhart et al., 1986) to find the optimal deterministic values of the weights and biases, BNNs treat them as random variables with probability distributions. BNNs uses Bayes' theorem, given in Eq. (6), to infer the posterior distribution of the weights and bias that is consistent with the training data set $D$. Hence their ability to quantify the uncertainty in their predictions through probabilistic outputs. Many techniques such as Markov Chain Monte Carlo (MCMC) methods (Gilks et al., 1995) can be used to sample from the posterior distribution of the weights, but they can be computationally expensive. This issue led to the development of approximations and more scalable methods, such as variational Bayesian inference (VI) (Blundell et al., 2015), probabilistic backpropagation (PBP) (Hernández-Lobato and Adams, 2015), Hamiltonian Monte Carlo (HMC) (Betancourt, 2017) and Bayesian dropout-based approaches (Gal and Ghahramani, 2016). While these methods have provided promising results, they also suffer from gradient-related problems such as vanishing and exploding gradients (Pascanu et al., 2013). Furthermore, they often force the model parameters $\theta$ (weights and bias) and the likelihood function to follow a predefined probability density function (PDF), typically Gaussian, which results in ignoring possible non-negligible multi-modalities of the posterior distribution (Ghahramani, 2015).

$$p(\theta \mid D, \mathcal{M}) = \frac{p(D \mid \theta, \mathcal{M})\, p(\theta \mid \mathcal{M})}{p(D \mid \mathcal{M})} \tag{6}$$

We explore a potential mitigation strategy of those issues with approximate Bayesian computation by subset simulation (ABC-SS) (Chiachio et al., 2014), using it as the Bayesian inference engine. ABC (Marin et al., 2012) is a computational Bayesian framework that avoids the formulation of the likelihood function $p(D \mid \theta, \mathcal{M})$, replacing it by forcing the probability of the prediction $\hat{y}$ to lie within a specific area $\mathcal{B}$ around the observed data $y$, based on a tolerance value $\epsilon$ which limits how far $\hat{y}$ can be from $y$ using a metric function $\rho$. Eq. (7) shows the new the posterior distribution of the parameters using the ABC formulation.

$$p_\epsilon(\theta, \hat{y} \mid D) \propto P\left(\hat{y} \in \mathcal{B}_\epsilon(y) \mid \theta\right) p(\hat{y}|\theta) p(\theta) \tag{7}$$

Additionally, the Subset Simulation technique (Au and Beck, 2001) enhances the efficiency of ABC during sampling, by transforming a rare event simulation problem into a sequence of nested simulations with larger probabilities and intermediate $\epsilon$ values. BNNs trained with ABC-SS (BNN by ABC-SS) were proposed in Fernández et al. (2022) and compared against the state-of-the-art BNNs in an experiment about fatigue in composite materials, providing comparable accuracy and a more flexible and non-parametric quantification of uncertainty. The success of this type of BNN lies in the non-parametric formulation of the PDF of the weights, the absence of likelihood function, and the fact that the gradient (partial derivatives) of a cost/likelihood function with respect to the model parameters does not need to be evaluated. BNN by ABC-SS was also combined with physics, into a hybrid model known as PG-BNN by ABC-SS (Fernández et al., 2023), which demonstrated to improve significantly the extrapolation capabilities of the neural network, and reduced the need for data.

## 3. Hybrid model for lithium-ion batteries trained with ABC-SS

In this section, the proposed Bayesian hybrid model and its implementation are described. This approach aims at harnessing the potential of ABC-SS to quantify the uncertainty in the observed data, the flexibility of artificial neural networks to capture non-linear patterns, and the knowledge and extrapolation capabilities of the physics-based Li-ion battery model.

The overall model architecture presented in this manuscript is inspired by the proposals in Nascimento et al. (2021), this is, two different MLPs are used to model the positive and negative non-ideal voltage $V_{ni,i}$, while the rest of the battery output voltage is given by the physics-based model, as per Eq. (1) in Section 2.1. Furthermore, the total resistance $R_o$ and the maximum charge $q_{max}$ are also considered as trainable parameters in the proposed hybrid model, being them correlated to aging effects as observed in previous studies (Daigle and Kulkarni, 2013). These two parameters have a considerable impact in the final voltage output of the model, and their value vary from battery to battery and throughout the life-span of each battery.

As explained in Section 2.1, a number of simplifications are used in the reduced order physics-based model, and the value of some elements, such as $V_{ni,i}$, $R_o$ and $q_{max}$, are fitted using experimental

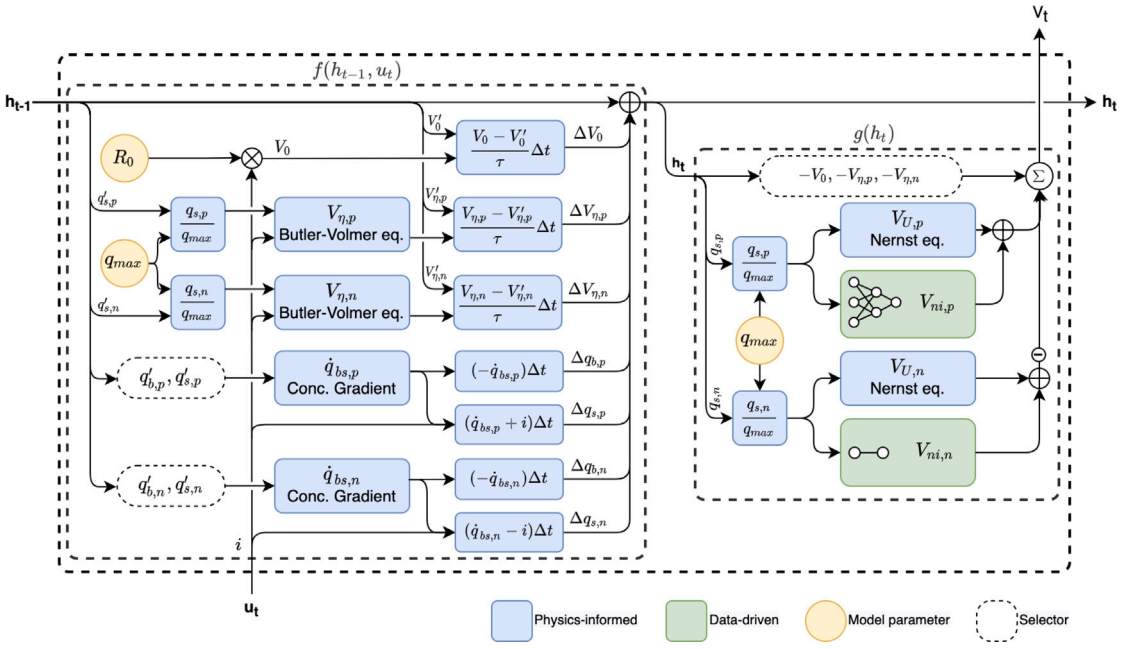


**Fig. 1.** Physics-informed RNN proposed in Nascimento et al. (2021).

data, which means that there exists an indeterminate amount of epistemic uncertainty. Indeed, both the data available to train the model parameters and our understanding of the complex physico-chemical processes that occur inside Li-ion batteries are limited. Moreover, the data collected during the experiments, which are then used to train the models, are subject to noise and possibly human errors. Therefore, quantifying the uncertainty in the outputs could be of great importance if these are to be used as inputs to other models in a wider system, or more generally, for any subsequent decision making-process.

In the following subsections, the pre-training and training of the hybrid model parameters using ABC-SS is explained. Also, the experiments undertaken are described and the results obtained are discussed.

### 3.1. Pre-training of the MLPs

Two MLPs are used to model the positive and negative non-ideal voltage $V_{ni,i}$, which are the correction terms required to calculate $V_{U,i}$, as per Eq. (3). The MLP for the positive side $V_{ni,p}$ comprises two hidden layers with 8 and 4 neurons respectively, tangent hyperbolic as the activation function in both layers, and a linear function for the output layer. The MLP for the negative side $V_{ni,n}$ has a simpler architecture with only one hidden layer and one neuron, using a linear function as the activation function. It should also be noted that the input data to the MLPs are normalized, and their outputs denormalized before they are introduced in $V_{U,i}$.

Given the formulation of the hybrid model, training the MLP for the positive side with random initialization render poor results. This is very common in neural networks, and was also observed in Nascimento et al. (2021). In addition, the training data is imbalanced, as the characteristic sudden drop in voltage when the battery is reaching the end of discharge is represented by around 5% of the total data only. This makes it difficult for the neural network to fit that section of the curve when ABC-SS is used and mean squared error (MSE) is chosen as the metric function $\rho$. The reason behind this issue lies in the rejection criteria of the ABC-SS algorithm, where a sample is accepted only if the value of its metric $\rho$ is lower than the intermediate tolerance $\epsilon_j$. This means that even if the last data points of the training curve are ignored, the sample can still achieve an acceptable average error, which translates in an overall good metric $\rho$ and therefore, be accepted. Moreover, the output from the positive MLP $V_{ni,p}$ is only a part of the total output voltage $V$ that is used to calculate the metric $\rho$ for each sample, being the rest defined by the physics-based model. Thus, the influence of the last points of the training curve in the overall metric $\rho$ is further diluted. The aforementioned issues can be solved by pre-training the MLPs with a synthetic curve.

The data created for pre-training is a 3-piece linear curve that approximates the decreasing non-ideal voltage given originally by the Redlich–Kister expansion. However, two different data sets are produced, one where the pre-training data points follow the same imbalanced distribution as per the training data, and another one where the pre-training data is distributed along the three sections of the piecewise linear curve in a way that there is a higher density of points in the last section. Also, two different metric functions are used, namely MSE and maximum absolute error (MaxE). This last metric is calculated by identifying the maximum absolute error made by the neural network among all training points. The hyperparameters used are: $N = 100{,}000$, $\rho$ = MSE/MaxE, $P_0 = 0.1$ and a Gaussian proposal function with an initial standard deviation $\sigma_0 = 1.5$ and a decrease rate of 0.5 per simulation level. No threshold $\epsilon$ is used, but instead the training process is done through 4 iterations of 10 simulations levels each, where the posterior distribution of the parameters at the end of one iteration becomes the prior distribution of the subsequent iteration. The results of the pre-training with the two data sets are shown in Fig. 2 where the following was observed:

- Panel (a): When data is imbalanced, using MaxE for the metric function provides better results. This is because the neural network is forced to minimize the error for every training data point individually, without taking into account the average error. That means that every point in the data set is equally important and needs to be fitted as closely as possible. Conversely, the results given by MSE are poor, given that closely fitting the first two sections of the curve was enough to achieve a low average error. That resulted in failing to fit the last part, which is arguably the most important one given that it is there where the voltage drops and defines the end of discharge.
- Panel (b): The increased density of data points in the last section of the pre-training curve forces the neural network trained with MSE to closely fit the whole length of the curve, as only fitting the first two sections is no longer enough to reach a low average

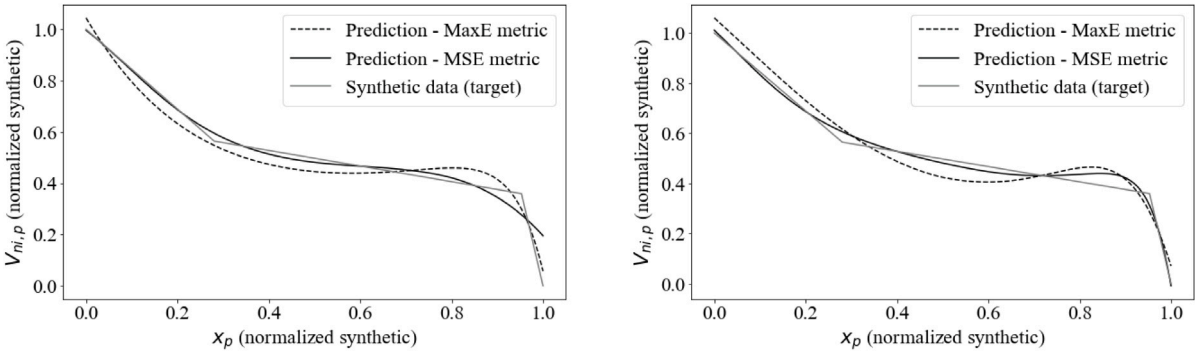


(a) Imbalanced data (b) Distributed data

**Fig. 2.** Pre-training of the MLP for the positive side. The continuous grey line represents the synthetic data, the dashed black line is the prediction of the MLP using MaxE as metric function, and the continuous black line refers to the prediction of the MLP with MSE as metric function. In panel (a) the pre-training synthetic data is imbalanced resembling the real battery data, while in panel (b) the pre-training data has been distributed to increase the density of points in the last drop of the curve. (For interpretation of the references to color in this figure legend, the reader is referred to the web version of this article.)

error. As expected, when MaxE is used as the metric function, the results are very similar to those achieved with imbalanced data.

Both approaches, MSE with balanced data and MaxE with either balanced or imbalanced data, have provided good results and could be used as the prior knowledge of the parameters when training the hybrid model. While MaxE has not provided better results than MSE with balanced data, it can be an alternative in those situations where the training data is imbalanced and pre-training with synthetic balanced data is not an option.

### 3.2. Training of hybrid model

The pre-training of the weights and bias of the MLP for the positive side was undertaken using ABC-SS as the learning engine, which means that the posterior distribution of the parameters after such stage becomes the prior distribution at the start of the subsequent training stage. The MLP for the negative side could also be pre-trained, however, this is not necessary and a using a standard Gaussian distribution $\mathcal{N}(0,1)$ as the prior distribution provided comparable results.

In order to train the proposed hybrid model with ABC-SS, the training algorithm proposed in Fernández et al. (2022) needs to be modified, given that now the parameters from two different MLPs along with the physical parameters $R_0$ and $q_{max}$ need to be adjusted. It seems sensible to expand the ABC-SS matrix to accommodate all the parameters in the hybrid model, and train them simultaneously. However, this approach renders the following two main issues:

- As explained in Section 2.3, ABC-SS is a Bayesian inference algorithm where the posterior distribution of the parameters is defined through iterative sampling and a rejection criteria. This sampling process is repeated through $\ell$ simulation levels, and $N$ samples are evaluated on each of them. As a result, training the overall hybrid model entails evaluating the training data set $N$ x $\ell$ times. The computational cost of training MLPs with ABC-SS is reasonable and comparable to that of backpropagation, as demonstrated in Fernández et al. (2022). However, the evaluation of the physics-based model lasts approximately one second, thus running the model for thousands of times to produce the full posterior distribution is prohibitive, and may take more than 27 h for this specific example.
- The number of samples $N$ required to train the MLPs with the Li-ion battery data sets is in the order of tens of thousands, thus even after the hybrid model was trained, the physics-based model would need to be evaluated $N$ times when making predictions on test data, or real data when the model was deployed. This would limit the applicability of the proposed hybrid model.

Thus, the main limitation of training the recurrent hybrid model with ABC-SS lies in the computational cost of running the physics-based model iteratively. To that end, the architecture of the recurrent cell is modified, by separating the MLPs from the physics-based models so they can be run independently. Also, a 2-stage training approach is proposed, where in the first stage the physical parameters are fixed and the MLPs are trained, and vice-versa for the second stage. This allows us to define a different number of samples $N$ for the MLPs and physical parameters, respectively $N_{MLP}$ and $N_{phy}$. Thus, the physics-based model only needs to be evaluated one single time when training the MLPs, and $N_{phy}$ times when training the physical parameters. The modified architecture is shown in Fig. 3, and the training process can be summarized as follows:

- First stage: The physical parameters $R_0$ and $q_{max}$ are fixed to default values of 0.117215 and 7600, respectively, from historical data and manufacturing specifications. Then, the MLP for the negative side is initialized with a standard Gaussian $\mathcal{N}(0,1)$ and the weights and bias of the MLP for the positive side, which were previously pre-trained, are loaded. Note that the number of samples $N_{MLP}$ is the same for both MLPs, and was defined at the pre-training stage. At this point, the hybrid model represented by the grey boxes in Fig. 3 is fully initialized and training starts. The physics-based battery model is run through all time steps of the training data only once, and three outputs are stored in separate arrays, namely the mole fractions $[x_p]_{t=1}^{t=T}$ and $[x_n]_{t=1}^{t=T}$, and the voltage $[V^*]_{t=1}^{t=T}$. This last element $V^*$ represents the total voltage without the correction terms $V_{ni,i}$, which are the outputs of the MLPs. Then both MLPs can be trained separately using ABC-SS as the learning engine and $[x_p]_{t=1}^{t=T}$ and $[x_n]_{t=1}^{t=T}$ as inputs. The weights and bias are adjusted based on the ABS-SS metric $\rho([\hat{V}]_{t=1}^{t=T}, [V]_{t=1}^{t=T})$, where $V$ represents the observed voltage and $\hat{V}$ is the predicted voltage, given by $\hat{V} = V^* + V_{ni,p} - V_{ni,n}$.
- Second stage: In the same way that $R_0$ and $q_{max}$ where fixed in the first stage, now it is the MLPs that are fixed, and to that end, the sample of weights and bias that provided the lowest training error in the first stage is selected. Then, the number of samples $N_{phy}$ for the physical parameters is defined, which is in the order of hundreds, instead of the tens of thousands used for the MLPs. The physical parameters are trained with ABC-SS, metric $\rho([\hat{V}]_{t=1}^{t=T}, [V]_{t=1}^{t=T})$, and following the forward pass shown in Fig. 3. To complete this second stage, the physics-based battery model needs to be run only $N_{phy}$ x $\ell$ times.

With the proposed architecture and phased training process, the computational cost and training time is reduced to 23 min approximately, which is comparable to the 21 min that takes the original

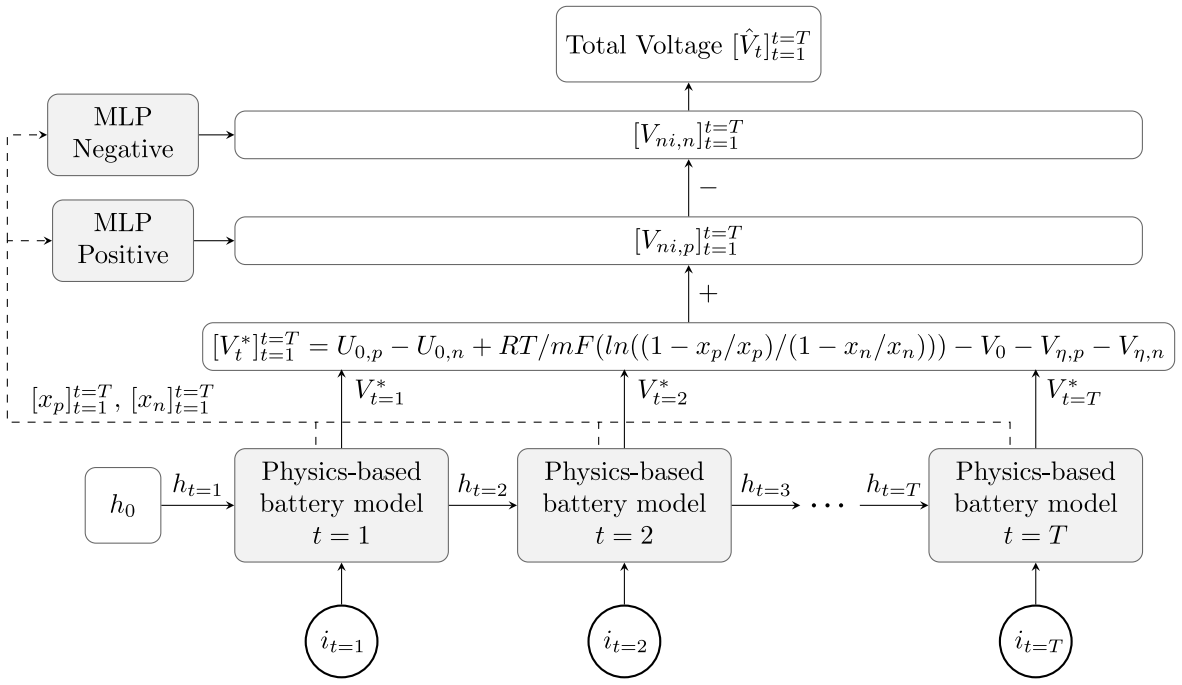


**Fig. 3.** Schematic representation of the folded and unfolded RNN.

architecture in Fig. 1 with backpropagation. This training time depends heavily on the number of samples and simulation levels, thus finer tuning of those hyperparameters might help to reduce the computational cost. Furthermore, if the samples were run in parallel with several processors the training process could be accelerated significantly.

Once the hybrid model is trained, predictions on test/validation data are made to evaluate its performance. Because of the 2-stage training and the modified architecture, when the overall model is assembled with all trained parameters, it means that the output of the hybrid model will have a dimension $T$ $x$ ($N_{MLP}$ $x$ $N_{phy}$), and again, the computation cost of running the full model escalates. To solve this issue, the resulting joint distribution of the physical parameters is described by 5 different features, namely their percentiles $P_5$, $P_{50}$, $P_{95}$, the sample with the lowest training error, and the sample with the highest training error. Thereby, the physics-based model only needs to be evaluated 5 times when making predictions on test data. While those features do not fully represent the overall joint distribution, they provided an acceptable approximation given the quasi-lineal behavior of the physical parameters $R_0$ and $q_{max}$.

The proposed multi-stage training method also allows us to quantify the uncertainty in the MLPs and the physical parameters separately. While some uncertainty may be shared between them, given that during training they would also try to compensate for the other, this is considered a reasonable approximation based on the information available. The only way to completely isolate the uncertainty from each parameter would be if the *real* values of $R_0$, $q_{max}$, $V_{ni,p}$ and $V_{ni,n}$ where known. In Section 3.3 the quantification of the uncertainty is shown and discussed. Finally, it is worth noting that the proposed architecture in Fig. 3 is fully compatible with gradient-based methods.

### 3.3. Experiments and results

The battery usage data utilized in this experimental framework is publicly available and can be found in Saha and Goebel (2007), Bole et al. (2014). These data have been extensively used in the field of prognostics applied to Li-ion battery, thus only the main characteristics are explained in this section. All batteries comprise a single cell, and their discharge profiles are recorded from a fully charged state with approximately 4.2 V to the point in which the voltage drops below 3.2 V, when the battery is considered to be discharged. Two types of tests were performed, using constant loading with 1 A current draw, and another with random loading where the current varied between 1 A and 4 A following a uniform distribution $i = U[1,4]$. In this manuscript, data from batteries 2, 3 and 4 are used. Specifically, 1 constant discharge curve and 2 random discharge curves are used for training, and then 1 of each type are used for testing. The reason behind this particular choice of training curves is an attempt to reproduce a real-world scenario, where the battery is first characterized with a constant discharge cycle, and then iteratively trained with such first curve and data coming from random discharge curves as they become available. The first curves from the repository are selected, so the aging effects are not yet present in the data.

A hyperparameter sensitivity analysis was carried out, so their optimal value can be selected based on their impact in the performance of the hybrid model when evaluated on a hold-out validation data set, consisting of a constant discharge curve different from the training and testing data sets. In terms of architecture of the MLPs, this was covered in previous Sections 3.1 and 3.2, and are the same as per the deterministic version used in Nascimento et al. (2021), so we can compare and evaluate if the accuracy remains in the same order of magnitude. Regarding the model hyperparameters, generally it is observed that for more complex architectures the number of samples $N$ needs to be increased, opposite to $P_0$ that needs to be smaller. The values for $\sigma_0$ and $p$, which affect the proposal function and how new samples are drawn, need to be adjusted simultaneously and iteratively. The tolerance value $\epsilon$ defines when the simulation stops, thus low values will potentially result in more accuracy, but will also affect the quantification of the uncertainty and require more simulation levels. Specifically in this case study, the following values of the model hyperparameters (MLPs) were used: $N_{MLPs}$ = 100,000, $\rho$ = MSE, $P_0$ = 0.1, threshold $\epsilon$ = 0.00056, and a standard Gaussian proposal function with an initial standard deviation $\sigma_0$ = 1.5 and a decrease rate of 0.5 per simulation level. The hyperparameters used to train the physical parameters are: $N_{phy}$ = 500, $\rho$ = MSE, $P_0$ = 0.5, threshold $\epsilon$ = 0.00024, initialization of $R_0$ = 0.117215, initialization of $q_{max}$ = 7600, and again a standard Gaussian proposal function with an initial standard deviation of 10% of the initial value of the physical parameters, and a decrease rate of 0.5 per simulation level.

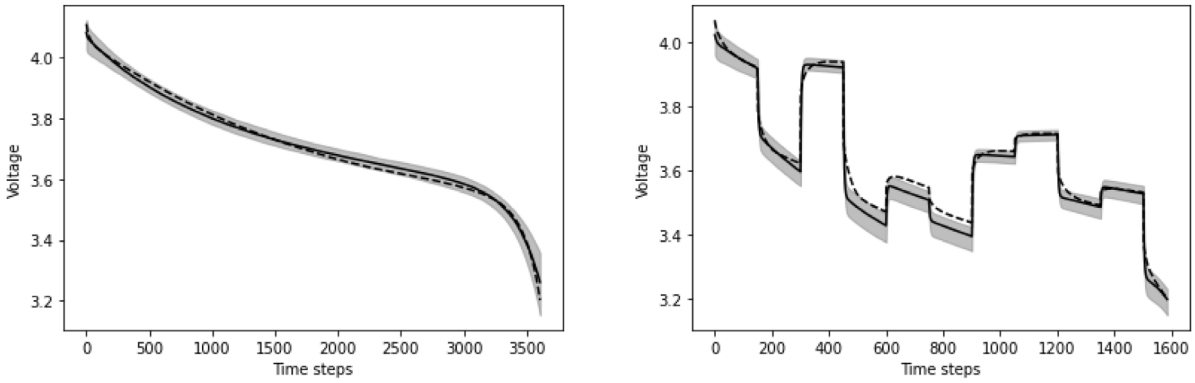


(a) Constant discharge (b) Random discharge

**Fig. 4.** Predictions on constant and random discharge test data made by the proposed hybrid model, trained with data from battery 3. The dashed-black line shows the measured (experimental) data, and the solid black line with the shaded grey area represents the average of the prediction with 90% confidence band. (For interpretation of the references to color in this figure legend, the reader is referred to the web version of this article.)

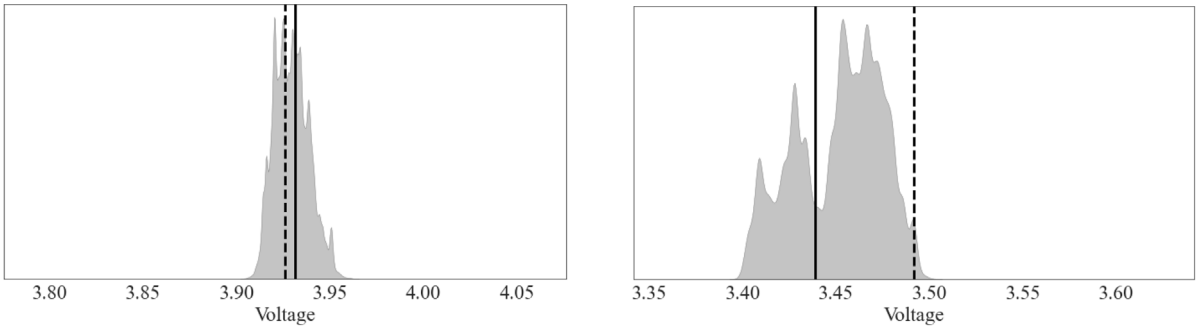


(a) Prediction at time step 340 (b) Prediction at time step 550

**Fig. 5.** Predictions made by the proposed hybrid model on random discharge test data, as per panel (b) in Fig. 4, at different time steps. The dashed-black line shows the measured (experimental) data, and the shaded grey area with the solid black line represent the probabilistic prediction and the average value respectively. (For interpretation of the references to color in this figure legend, the reader is referred to the web version of this article.)

The results obtained by the proposed method, in terms of accuracy, are shown in Table 1. It can be seen that the RMSE obtained for the three batteries are acceptable, and comparable to those achieved by the hybrid model in Nascimento et al. (2021), with the architecture shown in Fig. 1 and trained with standard backpropagation, reportedly 0.055 V in average and below 0.088% of the true voltage. The accuracy obtained by the pure physics-based model in Daigle and Kulkarni (2013) is not far from those values either. In any case, the results from the proposed method could be improved if the threshold $\epsilon$ was set to a lower value, prompting the Bayesian neural network to undertake further simulation levels. However, this would be detrimental for the quantification of the uncertainty, given that the diversity of samples would decrease in favor of a greater representation of the samples with lower training error. This is a trade-off inherited from the principles of ABC-SS, where the user needs to tune $\epsilon$ to find the right balance between precision and a good representation of the uncertainty present in the observed data. Being ABC-SS a gradient-free training algorithm, weights and bias parameters are updated probabilistically according to Bayesian principles, instead of using partial derivatives like in the traditional training method with backpropagation. This removes problems such as *"vanishing gradient"* or *"Dying ReLU"* without the need for more complex architectures like *LSTM* with gated units.

Fig. 4 shows predictions and uncertainty bounds against the test data for both constant and random discharge cycles. As can be seen, the uncertainty bounds enclose the majority of the test data points. Furthermore, it is observed that such uncertainty varies in different sections of the curves, and it is often greater in those parts where the prediction is less accurate. This can also be understood as a measurement of credibility, where narrower uncertainty bounds might be related to more accurate predictions, and vice-versa.

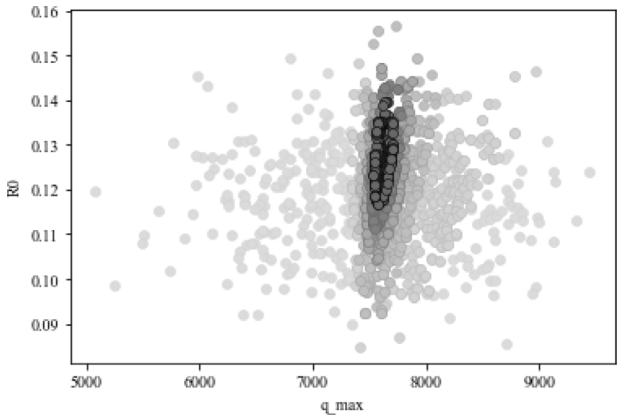


**Fig. 6.** Scatter plot of physical parameters samples drawn on each simulation level during training with data from battery 3. The different simulation levels are represented by different shades of grey, from light grey for simulation level 1 to dark grey for simulation level 6. (For interpretation of the references to color in this figure legend, the reader is referred to the web version of this article.)

A closer look at the uncertainty in the predictions is shown in panels (a) and (b) of Fig. 5, which represent a cross-section of panel (b) in Fig. 4 at time steps 340 and 550. It can be seen that the uncertainty

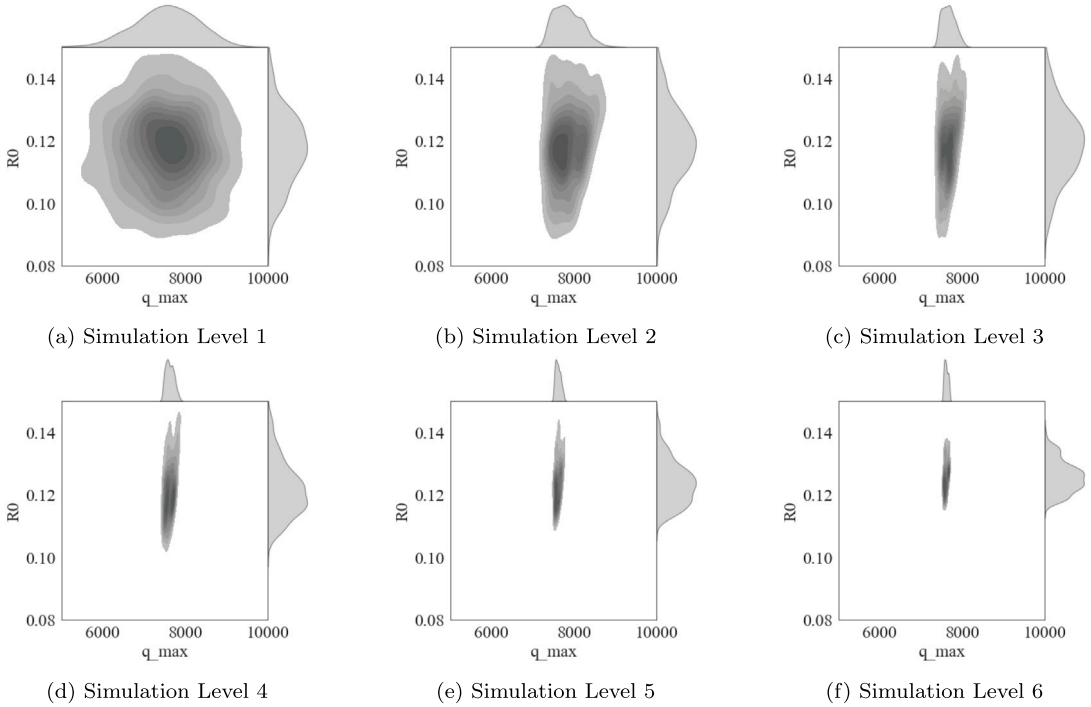


(a) Simulation Level 1 (b) Simulation Level 2 (c) Simulation Level 3

(d) Simulation Level 4 (e) Simulation Level 5 (f) Simulation Level 6

**Fig. 7.** Evolution of the joint distribution of the physical parameters through the different simulation levels during training with data from battery 3.

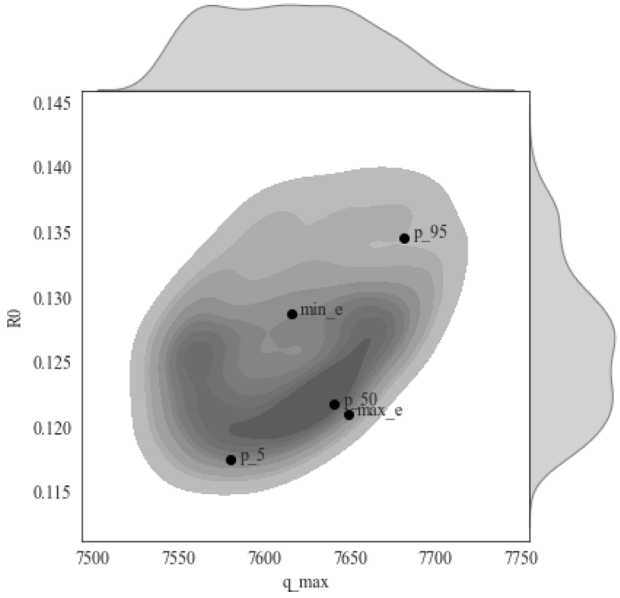


**Fig. 8.** Final joint distribution of physical parameters after training with data from Battery 3.

**Table 1**
Accuracy of the proposed method when tested on random discharge data.

| | Battery 2 | Battery 3 | Battery 4 |
|---|---|---|---|
| RMSE [V] | 0.0434 | 0.0392 | 0.0327 |

in panel (b) is approximately double than in panel (a), where the prediction is clearly more accurate. This is a good example of how the proposed Bayesian neural network conveys information about its trust, or lack of trust, in its own predictions. This uncertainty depends on several factors, such us variability or lack of training data points near the region of the test data point.

The proposed training method also provides information about the uncertainty in the MLPs and physical parameters $R_0$ and $q_{max}$; their distributions can be monitored through the different simulation levels. Fig. 6 shows a scatter plot of all the samples $N_{phy}$ of the physical parameters drawn in each simulation level during training with data from battery 3, using different shades of grey. This is a very representative image of ABC-SS training, where the prior information is updated simulation after simulation and the posterior distribution becomes more and more accurate, until it reaches the predefined threshold $\epsilon$ and the training stops.

The individual and joint distributions of the physical parameters throughout the different simulations are provided in Fig. 7, where we see more clearly how the joint posterior distribution starts from a prior Gaussian function, and it is updated step by step to reach its final form. The relation between $R_0$ and $q_{max}$ can also be read from those figures. Finally, Fig. 8 shows the final joint distribution of the physical parameters after training, along with the features used to represent it when making predictions on test data, as explained in Section 3.2. It can be seen that the distributions of the physical parameters inferred by the proposed Bayesian training is consistent with the information available from historical data and manufacturing specifications. The median value of the PDF inferred for $q_{max}$ is 7593, with plausible values ranging from 7568 to 7668. Considering that the starting point was anything between 6840 and 8360 (panel (a) in Fig. 7), the inferred distribution is close to the default value of 7600. The same applies to $R_0$ with a median value of 0.127, which again is close to the default value of 0.117. In this case, panel (f) in Fig. 7 shows more uncertainty about the value of $R_0$ than $q_{max}$. It should also be noted that the quality of the prior information may affect the limits of the search space in the first simulation level, as this would need to be larger in case the initial guesses were far from the target values. Nevertheless, vague prior information is not an issue, as setting the initial standard deviation $\sigma_0$ of the proposal function in ABC-SS to a high value ensures a comprehensive exploration of the parameter space. Equally, a high decrease rate may help to accelerate convergence.

In summary, training hybrid models with ABC-SS provided us with valuable information about the uncertainty in the predictions, which not only translates into a range of plausible values but also provides us with a measure of confidence in the predictions. Additionally, monitoring the joint distribution of parameters with ABC-SS conveys information about their relationship and importance in the overall model relative to each other. Thus, it may also be used to undertake a sensitivity analysis among the model parameters. Lastly, a series of drawbacks have also been unveiled, mostly related to the computational cost of the training method. But these issues are not specific of ABC-SS but common to any inference algorithm based on iterative sampling, such as Markov chain Monte Carlo (MCMC) methods. The use of parallel computation may also help to reduce the computational resources needed.

## 4. Conclusions

The demand for Li-ion batteries is increasing at a fast pace, mostly due to a surge in electric vehicles that use them for powering their engines, or operating their systems. For that very reason, new algorithms are constantly being developed to model the behavior and performance of these batteries. Among those, PINNs are a promising line of research, as they benefit from both physics-based knowledge and data-driven approaches.

In this manuscript, a new Bayesian PINN is proposed, where the recurrent architecture presented in Nascimento et al. (2021) was modified and adapted to be trained with ABC-SS instead of backpropagation. This Bayesian training method provides non-parametric weights, and avoids the formulation of a likelihood function, as well as the evaluation of its gradient. Those advantages translate into flexibility to adapt to the training data, and a realistic and coherent quantification of the uncertainty. Nonetheless, the method still poses some challenges, such as the difficulties found to fit the last part of the non-ideal voltage curve during pre-training, or the computational inefficiencies during training and testing. Regarding pre-training, balancing the training data and/or using maximum absolute error as the metric function in ABC-SS proved to solve the issue satisfactorily. With respect to the computational inefficiencies, adjusting the recurrent cell architecture so the data-driven and physics-based parts could be run separately clearly accelerated the training process. Furthermore, thanks to a multi-stage training approach, the physical parameters and the weights of the MLPs could be trained independently, which not only improved the computational cost of the hybrid model but also allowed for the uncertainty related to each type of parameter to be quantified in semi-isolation. This may also cast light into the relative importance of each parameter with respect to the others, with the potential to become a tool to evaluate the sensitivity of the model parameters. The experiment section demonstrated the accuracy of the proposed method, comparable to the standard backpropagation algorithm, as well as its ability to capture the uncertainty within the training data in a realistic manner.

Regarding future work, further research should undertaken about the aging effect in Li-ion batteries and how to include them in the proposed Bayesian hybrid model. Also, parallel computing should also be tested for the sampling stage, as it could also help to further reduce the overall computational cost of running the hybrid model.

## CRediT authorship contribution statement

**Juan Fernández:** Conceptualization, Methodology, Writing – original draft, Formal analysis, Software, Validation, Investigation, Visualization. **Matteo Corbetta:** Writing – review & editing, Investigation, Supervision, Validation, Resources. **Chetan S. Kulkarni:** Writing – review & editing, Supervision, Investigation, Resources. **Juan Chiachío:** Supervision, Investigation. **Manuel Chiachío:** Investigation, Resources, Project administration, Funding acquisition.

## Declaration of competing interest

The authors declare the following financial interests/personal relationships which may be considered as potential competing interests: Manuel Chiachio Ruano reports financial support was provided by European Commission Marie Sklodowska-Curie Actions.

## Data availability

Data is publicly available, the code is confidential.

## Acknowledgments

This paper is part of the ENHAnCE project, which has received funding from the European Union's Horizon 2020 research and innovation programme under the Marie Skłodowska-Curie grant agreement No 859957. The work by Matteo Corbetta and Chetan Kulkarni was supported under NASA Ames Research Center, Contract No. 80ARC020D0010. The authors would also like to thank the System-Wide Safety project and the Diagnostics and Prognostics Group at NASA Ames Research Center for the resources provided.

## References

Abadi, M., Agarwal, A., Barham, P., Brevdo, E., Chen, Z., Citro, C., Corrado, G.S., Davis, A., Dean, J., Devin, M., Ghemawat, S., Goodfellow, I., Harp, A., Irving, G., Isard, M., Jia, Y., Jozefowicz, R., Kaiser, L., Kudlur, M., Levenberg, J., Mané, D., Monga, R., Moore, S., Murray, D., Olah, C., Schuster, M., Shlens, J., Steiner, B., Sutskever, I., Talwar, K., Tucker, P., Vanhoucke, V., Vasudevan, V., Viégas, F., Vinyals, O., Warden, P., Wattenberg, M., Wicke, M., Yu, Y., Zheng, X., 2015. TensorFlow: Large-scale machine learning on heterogeneous systems. Software available from tensorflow.org.

Au, S.-K., Beck, J.L., 2001. Estimation of small failure probabilities in high dimensions by subset simulation. Probabilistic Eng. Mech. 16 (4), 263–277.

Berri, P.C., Dalla Vedova, M.D., Mainini, L., 2021. Computational framework for real-time diagnostics and prognostics of aircraft actuation systems. Comput. Ind. 132, 103523.

Betancourt, M., 2017. A conceptual introduction to Hamiltonian Monte Carlo. arXiv preprint arXiv:1701.02434.

Blundell, C., Cornebise, J., Kavukcuoglu, K., Wierstra, D., 2015. Weight uncertainty in neural network. In: International Conference on Machine Learning. PMLR, pp. 1613–1622.

Bole, B., Kulkarni, C., Daigle, M., 2014. Randomized battery usage data set. NASA AMES Prognostics Data Repository 70.

Cheng, Y., Song, D., Wang, Z., Lu, C., Zerhouni, N., 2020. An ensemble prognostic method for lithium-ion battery capacity estimation based on time-varying weight allocation. Appl. Energy 266, 114817.

Chiachio, M., Beck, J.L., Chiachio, J., Rus, G., 2014. Approximate Bayesian computation by subset simulation. SIAM J. Sci. Comput. 36 (3), A1339–A1358.

Coll, R.K., Lajium, D., 2011. Modeling and the future of science learning. In: Models and Modeling: Cognitive Tools for Scientific Enquiry. Springer, pp. 3–21.

Daigle, M.J., Goebel, K., 2012. Model-based prognostics with concurrent damage progression processes. IEEE Trans. Syst., Man, Cybern.: Syst. 43 (3), 535–546.

Daigle, M., Kulkarni, C.S., 2013. Electrochemistry-based battery modeling for prognostics. In: Annual Conference of the PHM Society, Vol. 5. (1).

Diampovesa, S., Hubert, A., Yvars, P.-A., 2021. Designing physical systems through a model-based synthesis approach. example of a li-ion battery for electrical vehicles. Comput. Ind. 129, 103440.

Doyle, M., Fuller, T.F., Newman, J., 1993. Modeling of galvanostatic charge and discharge of the lithium/polymer/insertion cell. J. Electrochem. Soc. 140 (6), 1526.

Fernández, J., Chiachío, J., Chiachío, M., Barros, J., Corbetta, M., 2023. Physics-guided bayesian neural networks by abc-ss: Application to reinforced concrete columns. Eng. Appl. Artif. Intell. 119, 105790.

Fernández, J., Chiachío, M., Chiachío, J., Muñoz, R., Herrera, F., 2022. Uncertainty quantification in neural networks by approximate Bayesian computation: Application to fatigue in composite materials. Eng. Appl. Artif. Intell. 107, 104511.

Fleischmann, J., Hanicke, M., Horetsky, E., Ibrahim, D., Jautelat, S., Linder, M., Schaufuss, P., Torscht, L., van de Rijt, A., 2023. Battery 2030: Resilient, sustainable, and circular. McKinsey Glob. Battery Alliance.

Gal, Y., Ghahramani, Z., 2016. Dropout as a bayesian approximation: Representing model uncertainty in deep learning. In: International Conference on Machine Learning. PMLR, pp. 1050–1059.

Ghahramani, Z., 2015. Probabilistic machine learning and artificial intelligence. Nature 521 (7553), 452–459.

Gilks, W.R., Richardson, S., Spiegelhalter, D., 1995. Markov Chain Monte Carlo in Practice. CRC Press.

Haley, P.J., Soloway, D., 1992. Extrapolation limitations of multilayer feedforward neural networks. In: [Proceedings 1992] IJCNN International Joint Conference on Neural Networks, Vol. 4. IEEE, pp. 25–30.

Hernández-Lobato, J.M., Adams, R., 2015. Probabilistic backpropagation for scalable learning of bayesian neural networks. In: International Conference on Machine Learning. PMLR, pp. 1861–1869.

Karthikeyan, D.K., Sikha, G., White, R.E., 2008. Thermodynamic model development for lithium intercalation electrodes. J. Power Sources 185 (2), 1398–1407.

Marin, J.-M., Pudlo, P., Robert, C.P., Ryder, R.J., 2012. Approximate Bayesian computational methods. Stat. Comput. 22 (6), 1167–1180.

Nascimento, R.G., Corbetta, M., Kulkarni, C.S., Viana, F.A., 2021. Hybrid physics-informed neural networks for lithium-ion battery modeling and prognosis. J. Power Sources 513, 230526.

Ning, G., Popov, B.N., 2004. Cycle life modeling of lithium-ion batteries. J. Electrochem. Soc. 151 (10), A1584.

Pascanu, R., Mikolov, T., Bengio, Y., 2013. On the difficulty of training recurrent neural networks. In: International Conference on Machine Learning. PMLR, pp. 1310–1318.

Petrillo, A., Picariello, A., Santini, S., Scarciello, B., Sperli, G., 2020. Model-based vehicular prognostics framework using big data architecture. Comput. Ind. 115, 103177.

Raissi, M., Perdikaris, P., Karniadakis, G.E., 2019. Physics-informed neural networks: A deep learning framework for solving forward and inverse problems involving nonlinear partial differential equations. J. Comput. Phys. 378, 686–707.

Rong, P., Pedram, M., 2006. An analytical model for predicting the remaining battery capacity of lithium-ion batteries. IEEE Trans. Very Large Scale Integr. (VLSI) Syst. 14 (5), 441–451.

Rumelhart, D.E., Hinton, G.E., Williams, R.J., 1986. Learning representations by back-propagating errors. Nature 323 (6088), 533–536.

Saha, B., Goebel, K., 2007. Battery data set. NASA AMES Prognostics Data Repository.

Shi, J., Rivera, A., Wu, D., 2022. Battery health management using physics-informed machine learning: Online degradation modeling and remaining useful life prediction. Mech. Syst. Signal Process. 179, 109347.

Tang, T., Yuan, H., 2022. An indirect remaining useful life prognosis for li-ion batteries based on health indicator and novel artificial neural network. J. Energy Storage 52, 104701.

Vaish, R., Dwivedi, U., Tewari, S., Tripathi, S.M., 2021. Machine learning applications in power system fault diagnosis: Research advancements and perspectives. Eng. Appl. Artif. Intell. 106, 104504.

Venugopal, P., Shankar, S.S., Jebakumar, C.P., Agarwal, R., Alhelou, H.H., Reka, S.S., Golshan, M.E.H., 2021. Analysis of optimal machine learning approach for battery life estimation of li-ion cell. Ieee Access 9, 159616–159626.

Wen, P., Ye, Z.-S., Li, Y., Chen, S., Zhao, S., 2023. Fusing models for prognostics and health management of lithium-ion batteries based on physics-informed neural networks. arXiv preprint arXiv:2301.00776.

Yucesan, Y.A., Viana, F.A., 2021. Hybrid physics-informed neural networks for main bearing fatigue prognosis with visual grease inspection. Comput. Ind. 125, 103386.